Journal of Coastal Research	37	4	716–725	Coconut Creek, Florida	July 2021

A Dynamic Marine Oil Spill Prediction Model Based on Deep Learning

Renda Wang[†]*, Zhen Zhu[†], Wei Zhu[†], Xianping Fu[‡], and Shengwei Xing[†]

[†]Navigation College
Dalian Maritime University
Liaoning, China

[‡]Information Sciences and Technology College
Dalian Maritime University
Liaoning, China

www.cerf-jcr.org

www.JCRonline.org

ABSTRACT

Wang, R.; Zhu, Z.; Zhu, W.; Fu, X., and Xing, S., 2021. A dynamic marine oil spill prediction model based on deep learning. *Journal of Coastal Research,* 37(4), 716–725. Coconut Creek (Florida), ISSN 0749-0208.

Water pollution resulting from shipborne oil spills has caused tremendous damage to local marine ecology and has led to huge property losses. By establishing a multi-angle monitoring and early-warning mechanism, the oil spill's trajectory to a large extent can be effectively predicted, and thereby the accompanying economic losses can be reduced. In this study, real-time processing is performed on an oil spill monitoring video frame to analyze the characteristics of the spilled oil, such as the edge contour features, diffusion rate, centroid, area, *etc*. An initial system model and an oil spill behavior monitoring model were established based on the previously mentioned characteristics. A long short-term memory network in a recurrent neural network was introduced to deal with the memory information to obtain the connection between features and influencing factors. The spatial variable distribution of a dynamic grid reference system, as a substitution of the traditional original data sequence, was used as the system input. The result shows that the model has good stability and can provide a reliable interactive prediction; the result is especially significant given the vigorous exploitation of petroleum resources and the rapid development of maritime transportation in today's global economy. The auxiliary oil spill early-warning system investigated in this paper provides a scientific basis for targeted strategic oil spill emergency planning.

ADDITIONAL INDEX WORDS: *Image processing, long short-term memory, artificial intelligence, behavioral dynamic prediction.*

INTRODUCTION

The environmental and economic losses caused by the occurrence of offshore oil spills are huge. The international community has some practical experience in emergency response to offshore oil spills. From 1988 to 1991, 28 oil spills of 500,000 L (132,100 gal) or more occurred (Yapa, 1996). The total volume of oil spilled from a major spill, excluding the Arabian Gulf/Kuwait spill, for the same period was 293,000,000 L (77,400,00 gal). The 1991 Arabian Gulf/Kuwat spill was estimated at 143 billion L (37.8 billion gal). Improving the accuracy of the detection of the oil spill influence range and the reliability of dynamic path prediction for oil spills is essential. The current detection and prediction methods include traditional remote sensing technology and hyperspectral and polarized oil spill remote sensing to improve the monitoring of oil spill accidents (Bhangale *et al*., 2017; Garcia-Pineda *et al*., 2019; Pisano *et al*., 2016). The use of surface drift buoys and GPS positioning technology provides a eal-time environmental monitoring and oil spill drift trajectory tracking (Abascal *et al*., 2017; Chiri *et al*., 2019). Through the application of synthetic-aperature radar echo signal images, a semi-automatic classification method is adopted to combine with GIS system processing to analyze and evaluate the distribution range, diffusion factors, and impact on the surrounding environment of oil spill (Alpers, Holt, and Zeng, 2017; Garcia-Pineda *et al*., 2017; Xiong and Zhou, 2019). An oil spill warning system based on fluorescence spectroscopy is used to study the fluorescence spectrum characteristics of different oil spill types, which provides a method to quickly distinguish the degree of oil spill pollution (Hou *et al*., 2019; Mirnaghi *et al*., 2019; Zhang *et al*., 2019). Mansur and Price (2019) established a sea oil spill model of the oil film under the action of tides and wind waves by combining the hydrodynamic mathematical model and proposed the motion equations of oil film diffusion, evaporation, and emulsification expressed in the form of differential equation. Ji *et al*. (2020), Yu (2019), and Zhang *et al*. (2020) established a deep-sea oil spill model based on the Lagrange integral method, which can simulate or predict the temporal and spatial distribution of oil pollutants in the marine environment and can also provide decision-making choices for pre-accident risk assessment and emergency response support.

These methods have improved the ability to monitor oil spills to varying degrees. However, the general detection process is relatively complex and time delayed. It generally stays only in the aspect of oil spill detection and rarely involves dynamic prediction of real-time oil spill behavior for edge contour features. Humans will eventually evolve to unknown scenes to make up for its longer reaction time. It is the most effective auxiliary method for motion prediction to improve the robustness and real-time nature of the early-warning system by increasing the system's proactive perception and predictive planning capabilities (Mao *et al*., 2019). Neural networks have powerful image processing capabilities that can identify and predict the dynamic behavior of image to a large extent. The

DOI: 10.2112/JCOASTRES-D-20-00080.1 received 16 June 2020; accepted in revision 27 November 2020; corrected proofs received 18 January 2021.

*Corresponding author: radar@dlmu.edu.cn

traditional recurrent neural network (RNN) structure is simple and uses a back propagation training algorithm (Sari, Wulandari, and Suprapto, 2019). The disadvantage of the algorithm is that when the training time is longer, the residuals returned by the system will be decreased exponentially, and the weight update will be slow. The proposed long short-term memory (LSTM) can effectively solve the problem of gradient dispersion in traditional recurrent network structures. The drift, diffusion rate, and influence range of oil spills can be further calculated by establishing a mathematical model of oil spills and adding real-time images to the experimental database and collecting edge contour features as well as applying a cyclic neural network algorithm to dynamically predict the images. Moreover, the established oil spill model has low equipment requirements and low detection cost, and it can be used as an auxiliary system for oil spill emergency mitigation and recovery plan, therefore providing a strong theoretical basis for accident monitoring and oil spill recovery.

METHODS

To establish a mathematical model of offshore oil spills, this paper observes the real-time, two-dimensional (2D) time series images obtained by analyzing the available silicon dioxide melting experiments in crucible of the same category when an offshore oil spill accident occurs. The experimental image data was added to the experimental database, and the edge contour features, such as the centroid, perimeter, area, and diffusion rate of the research object (Yankelovich and Spitzer, 2019), were collected to perform graphic analysis processing through the cyclic neural network algorithm. By tracking the centroid movement trajectory of the particles, an edge profile indication module and LSTM network learning were established to estimate the actual melting rate of silicon dioxide and dynamic prediction of behavior.

Establishment of the Initial Model

By combining the preprocessed 2D image data set with the improved central moment fast search algorithm, the data tracking model of the change of the centroid position during the melting process was calculated. According to the established mathematical model, the following edge profile characteristics of silicon dioxide were selected: shape (F), perimeter (L), concentration (C_b), diffusion rate (V_x), and area (S_v). To this end, this paper uses the LSTM networks algorithm in the RNN to analyze and predict the change trend of the region to ensure the accuracy of the experimental results (Jeong, Kim, and Yi, 2020). Then, this paper takes the Matplotlib tool of Python 3.7.1 to analyze the m-t relationship to obtain the melting rate of silicon dioxide and to complete the image analysis of the initial model. Silica undergoes a non-uniform state change in the molten state at ultrahigh temperature, and it has adhesion; only part of it is an extremely small, free distance state of particles. The melting process of silicon dioxide and the process of an oil spill at sea can be regarded as a reverse process. The research object of this article is the 2D image set during the oil spill process, and the goal of the research is to deduce the dynamic simulation trend of the Δt oil spill based on the initial image changes through neural network learning. According to the predicted trajectory, processing work such as containment can be performed in a targeted manner, and more rescue time can be obtained.

The 2D time series graphs in the experimental data set shows the fixed position of the crucible in the image and the change of the position information of the molten silicon dioxide particles with time. In reality, the reactions inside the blast furnace feature dynamic, nonlinear, and hysteretic impede accurate mathematical modeling (Ding *et al.*, 2017). Accordingly, the edge profile of the particles was characterized, and the actual melting rate of silicon dioxide was estimated. To confirm the positional change of silicon dioxide at high temperature, the edge profile feature was selected, and the real-time melting rate prediction of silicon dioxide was calculated. Then the solution of the initial model can be mapped to the diffusion range of oil leakage and the solution of the rate model when the offshore oil spill event occurs.

To simplify the problem and to make this model easy to be used in the training and testing, this paper made a basic assumption. As the particles continue to melt at high temperature, the particle image recognition obtained by the high, heat-resistant camera is gradually blurred. Therefore, it ignores the detection of micro-edge parts that cannot be recognized by the minimum resolution of the camera. The particles are very small, and it is assumed that the solid unit mass m_i of the particle surface is evenly distributed. The model ignores the non-uniform velocity change of the high-temperature melting rate caused by the external environment and the possible mathematical carry error. To track the volume change Y_y of the silicon dioxide at the time step H, data preprocessing is performed on the original 2D image, the spatial distribution change rate is used for prediction, and a grid-coordinate system with a specification of $n \times n$ is established. The center of mass of the silicon dioxide block is (x, y), which predicts the future state sequence group.

$$Y^{t+H} = k_j * g\left(X^{t+H}\right) + Z^i \tag{1}$$

where, X^{t+H} and Y^{t+H} are the X and Y coordinate positions of the mass point of the time step H, and the actual solution formula after analyzing X and Y is $x_j[m1(i), m2(i+1), \ldots, mn(I+H)]$, $y_j[m1(i), m2(i+1), \ldots, mn(I+H)]$.

In the process of extracting image edges from experimental materials, this paper uses an improved first-order absolute center moment search algorithm (Santiago *et al.*, 2019). As shown in Figure 1, S_1 and S_2 are the critical areas of the edge of the pixel, Fx and Fy are the corresponding window coordinate system. By taking the gray value of the pixel as the quality distribution of the point and taking the image center moment as the feature matching target, the particle centroid and the image edges can be obtained with less deviation in this experiment. It can work under low signal-to-noise ratio with high recognition accuracy and strong local anti-interference ability.

Prediction of the Dynamic Trend of Offshore Oil Spill

The marine oil spill process includes evaporation, dissolution, spreading, convection, emulsification, and other processes. The conventional numerical model uses different methods to establish the oil film expansion model, convection spreading model, and oil particle model. The calculation of each model

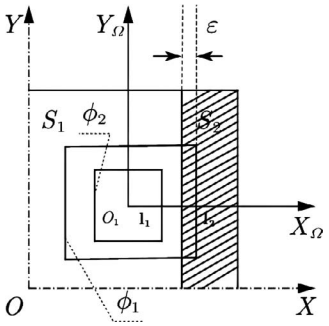

Figure 1. Sketch map of the algorithm, S_1 and S_2 are the critical areas of the edge of the pixel, *Fx* and *Fy* are the corresponding window coordinate system (*x*-*y*). This figure shows the schematic diagram of edge feature extraction method in the process of experiment. The pixel value is used as the edge processing object, and the central moment is used as the matching feature. It can get higher recognition accuracy and stronger antijamming ability in the environment with low signal noise ratio (SNR).

improves the accuracy of the marine spill oil process behavior prediction, but generally shortcomings such as weak generalization ability and poor visualization ability still occur.

This paper uses a relatively macroscopic method to do this research. The image data collected in the early stage of oil spill are used as input data. Through the intensive training of the neural network, the weight parameters can be obtained, which can well reflect the explicit or potential chain relationship between the various influencing factors and obtain the relative changes of various "strong action" and "weak effect" process represented by the hidden layer in the process of oil spill. Finally, the influence weight of evaporation, dissolution, and emulsification on the oil spill image is weakened by the obtained parameter values, and then the influence of oil particle diffusion and wind, temperature, convection, and other factors on the dynamic trajectory change of oil spill process is mainly studied in the time-varying process of image.

The general model of the RNN can solve the problems related to the time series relationship between $t-1$ and $t+1$, but the structure is relatively simple. The LSTM is a special RNN that is mainly used to solve the problem of gradient disappearance and gradient explosion in the training process similar to long sequence (Wang, Zhu, and Li, 2019). Compared with ordinary RNNs, LSTM does not simply perform memory overlap work, but it also controls the transmission status through gating logic settings so that it can perform better in a longer sequence.

Existing behavior tracking methods (ICT, GPS, RFID, *etc.*) usually use physical thinking. Generally speaking, the model is analyzed by a fixed coordinate system space segmentation method, and the general prediction is for the close-range mode of dynamic objects. For the other part, various position-aware device systems are used to track the movement of objects and to collect a large amount of spatiotemporal data. The results showed that the relatively limited prediction range leads to computational boundary restrictions, which makes it easy to ignore the data errors caused by the irregular diffusion of the density of objects. The introduction of the LSTM network prediction model can autonomously increase the regional influence variable *Xi*, add the number of hidden layers *Hi*, and adjust the weight coefficient *Wi* between each layer so that the system can simulate the adhesion and dependence of relevant parameters. The image processing method using artificial intelligence has large error tolerance, flexibility, and real-time performance, and the experimental results can be used as an auxiliary work of the oil spill early-warning system and have great reference value.

The oil spill dynamic prediction model uses the spatial distribution variable preprocessing of the dynamic grid reference system as the system input, which can well avoid the prediction offset problem caused by the delay of the multisensor processing of the original data. The system uses a RNN, and the algorithm can well handle the simulation of dynamic processing capabilities between complex interrelationships (such as the growth of static parts and the actual movement of objects).

Physical Experiments

The damage cycle caused by an oil spill is long, and the repair process is complicated. Only by accurately simulating and predicting the changes of the oil spill trajectory can emergency countermeasures better select and formulate to reduce the damage to the local ecological environment caused by the occurrence of oil spill accidents.

To further verify the feasibility of the model in predicting the an oil spill trajectory, this paper selects the deep-sea oil spill test with diesel-natural gas mixture as the leakage in the "DeepSpill" test set for the next numerical simulation study of the oil film (Murawski *et al.*, 2019). The project is a joint oil spill test conducted by the U.S. Mineral Resources Administration and 22 oil companies in the Norwegian waters from 27–29 June 2000. Regarding the problem of image sampling in the silica fusion experiment, this paper has added a detailed description of image sampling in the "Methods" section, including the data perform preprocessing, preprocessing, hourglass screening, approximate cutting, breakpoint detection, image deduction, and other processes. The analysis of the test results is used to prevent and respond to sudden deep-sea oil spill accidents by obtaining the data required for the verification of the oil spill model and by observing the monitoring equipment for deep-sea oil spill accidents and to evaluate the safety issues of deep-sea oil spill accidents. The experimental results are relatively complete and highly representative.

This paper mainly studies the change of the spatial distribution of oil film on the sea. First, the oil film is abstracted as a body comprising a large number of elliptical discretized "oil particles." The oil particle model divides the oil spill motion process into two main parts within the time Δt, namely the expansion process and the drift process. Because the expansion and drift process of the oil film is reflected in the size and spatial location of the oil particles, this experiment takes oil particles as the research object for experimental analysis. Through the collection of information on the marine environment of the DeepSpill experiment to study the specific impact of oil spills. As shown in Figures 2–4, the graph shows a smooth wind speed-wind direction curve and schematic diagram of sea temperature at the Helland Hansen station during the sea trial (the analysis of specific wind direction information is more complicated). Therefore, in this paper, the measured map of the

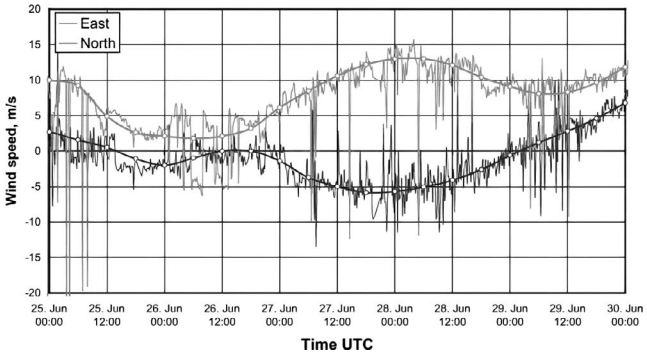

Figure 2. Schematic diagram of actual measured wind speed and direction with a lot of noise interference (v-t). The two factors that have the greatest influence on oil spill behavior in sea breeze information are shown: east wind and north wind. For the convenience of calculation, the extremely irregular wind direction and wind speed information are fitted into smooth curves, and the fitted data are input into sea wind factors according to the system trained test channel, as the prediction of oil spill dynamic behavior.

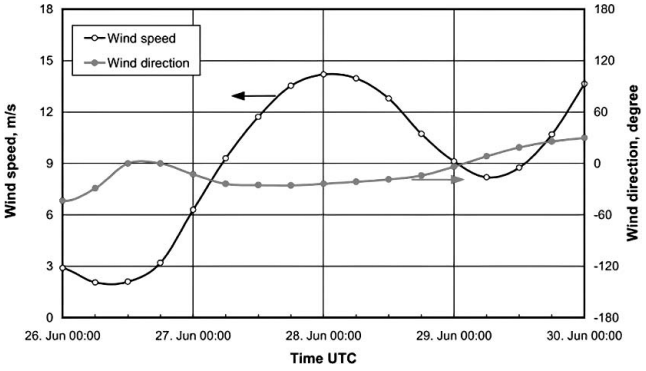

Figure 3. Smooth plot of wind speed and direction at the Helland Hansen site during the DeepSpill sea trial (*v*-*t*). After smoothing Figure 2, how to process the input of the system by extremely irregular sea breeze is shown; other processes are similar to this method.

marine environment in Figure 2 is simplified into the two most influential pieces of sea-breeze information, the east wind and the north wind, and finally the stable data are obtained.

Numerical Model

Assume that the total kinetic energy of the material object system is expressed as follows:

$$\vec{P} = \sum m_i v_i = m\vec{V}_C \tag{2}$$

$$\left.\begin{aligned} \overrightarrow{V_C} &= \frac{d\overrightarrow{r_c}}{d_t},\ \overrightarrow{V_i} = \frac{d\overrightarrow{r_i}}{d_t} \\ \overrightarrow{V_C} &= \frac{\sum m_i \overrightarrow{v_i}}{m} = \frac{\sum m_i \frac{d\overrightarrow{r_i}}{d_t}}{m} = \frac{\sum m_i d\overrightarrow{r_i}}{m} \end{aligned}\right\} \tag{3}$$

The centroid can also be called the average position of the mass distribution, that is, the position vector of the point is the average position of the mass of each point position vector of the point system. In the rectangular coordinate system, the expression of each component of the point is as follows:

$$X_c = \frac{\sum_{i=1}^{n} m_i x_i}{\sum_{i=1}^{n} m_i} \quad Y_c = \frac{\sum_{i=1}^{n} m_i y_i}{\sum_{i=1}^{n} m_i} \tag{4}$$

For a 2D continuous image, $f(x, y) \geq 0$; pq in the $p + q$ order matrix is a non-negative integer. For more discrete digital images, M_{pq} and the central moment μ_{pq} are defined as follows:

$$m_{pq} = \sum_{j=1}^{N} \sum_{x=1}^{N} i^p j^q f(i,j) \tag{5}$$

$$\mu_{\mathrm{pq}} = \sum_{j=1}^{N} \sum_{i=1}^{N} (i - i_c)^p (j - j_c)^q f(i,j) \tag{6}$$

where, (ic, jc) is the centroid coordinate. The centroid of the image is the 0th- and first-order moment. It is called a dynamic particle by taking any point on the image $f(i, j)$ as the initial point of the search procedure, which can be continuously modified from this point to the mass point of the target 2D image. Let $f(i, j)$ be the coordinates of the dynamic point. The sum of the distances from all the points on the image to the dynamic particles:

$$h(k,l) = \begin{cases} \sum_{j=1}^{N} \sum_{i=1}^{N} d(i-k, j-k) f(i,j) \\ \sum_{j=1}^{N} |j-l| f(i,j) + \sum_{i=1}^{N} |i-k| f(i,j) \\ h(k,x) + h(l,x) \end{cases} \tag{7}$$

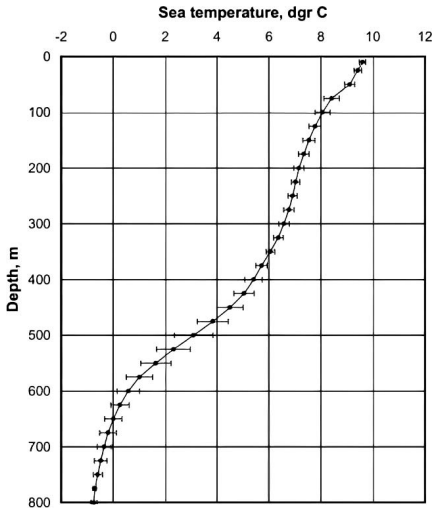

Figure 4. Simulated map of seawater temperature at the Helland Hansen site during the sea trial (*T*-*t*). In the image of temperature effect on oil spill process, the temperature changes of different depths are detected. With the increasing of ocean depth, the temperature drops sharply, but in the initial stage of the oil spill, the temperature change of ocean surface and within 100 m is relatively slow; therefore, the influence of temperature on oil particles can be correlated with random model, and the oil spill influence results closer to the natural law can be obtained.

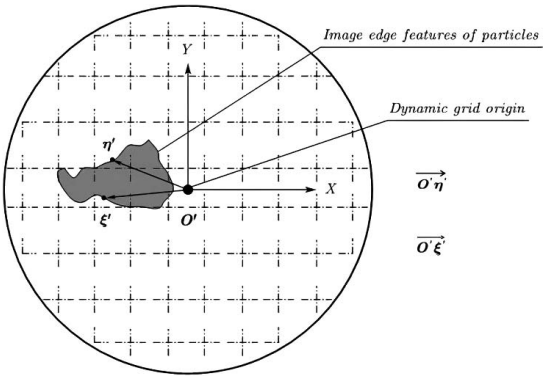

Figure 5. A total of 114 similar 2D experimental image data were collected in the time range of TÚ[0, 200], and the spatial variable distribution of a dynamic grid reference system, as a substitution of the traditional original data sequence, was used as the system input.

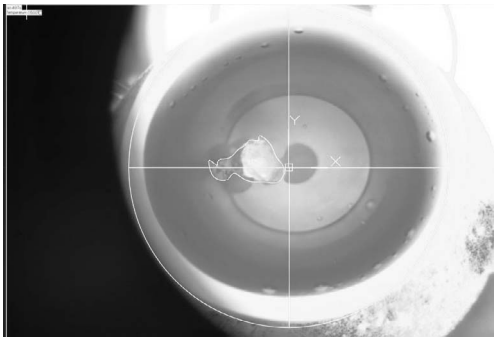

Figure 6. The internal template map of the model and the model edge contour diagram at $T = 10$ (s) were obtained through the central moment theory. Using this reference frame, we can capture the contour features of the initial model more quickly, which is conducive to the image processing of the dynamic changes of real objects and can increase the generalization ability of the whole preprocessing process.

Among them, $h(k, l)$ is the sum of the distances of all the target points, that is, the distance from the target point to $x = k$ and the vertical straight line $y = l$. As shown in Figures 5 and 6, a total of 114 similar 2D experimental image data were collected in the time range of $T \in [0, 200]$, and the internal template map of the model and the model edge contour diagram at $T = 10$(s) were obtained through the central moment theory.

When an oil spill accident occurs, it is usually accompanied by the expansion, drift, evaporation, dispersion, emulsification, and dissolution of the oil film (Kasimu, Wu, and Bian, 2019). Only by analyzing the marine environment and oil spill properties in time can it more accurately grasp and predict the dynamic trajectory of the oil spill behavior. When the oil spill mixture leaks into the designated sea area, in addition to the influence of gravity, viscosity, and surface tension on the self-expanding movement of the oil spill, the marine environment at that time, including wind speed and current, also had a large influence on the behavior. When the mixture is subjected to wind and currents, drift and diffusion will soon occur.

To further study the specific effects of wind V_w and ocean current V_F on an oil spill, the edge expansion displacement factor α and edge drift rate factor β are introduced based on the establishment of the initial oil spill model. At the same time, the spatial position calculation equation of oil film particles needs to be adjusted.

$$Z^{t+H} = X^{t+H} + jY^{t+H} \tag{8}$$

$$Z^n = \alpha Z^{t+H} + \frac{\beta \Delta t}{2} + \Delta Z_r \tag{9}$$

Among them, Z^{t+H} is the space position vector in Δt time, Z^n is the oscillation displacement after adding wind and influencing factors of seawater flow, and ΔZ_r is the random walk distance of oil particles at fixed points.

In this paper, to study the influence of wind and flow forces on particles in the dynamic grid-reference coordinate system, it is assumed that the effect of wind and flow forces on particles can be regarded as a uniform effect in the process of image processing. This paper introduces random factors into the position of particles at time t under the constraint of Equations (8) and (9). On the premise of $\Delta t = 0$, the influence of wind and current forcing is considered to be a random result in a short period of time, which is also relatively consistent in the complex movement of oil particles in the actual oil spill environment. The real-time random number is obtained with a Pytorch tool, and the numerical value most in line with the natural change law is obtained by graphics processing unit acceleration to calculate the impact of both on particles. The randomness of these two factors needs only to consider the weight distribution of the two factors in a specific environment so that compared with other traditional methods, the influence of wind and ocean current on oil particles can be described more accurately and simply.

The occurrence of oil spills is uncertain at the time level, and the concentration trend of liquid diffusion is relatively vague; therefore, the environmental pollution problems are more serious (Nhat, Venkatatesan, and Khan, 2020). Only through the prediction of the target's diffusion trend and the scope of coverage and making accurate rescue planning can the most valuable oil spill cutoff time can be obtained. By assisting the offshore oil spill warning system to track the development trend of oil spill accidents, it can make a better scientific basis for the future oil spill recovery link. Based on the establishment of the silicon dioxide model in the first two sections, the schematic diagram of the dynamic prediction system of the LSTM network's behavior in the event of an offshore oil spill was described, which provided a theoretical support for the realization of the model.

RESULTS

This paper first focuses on the establishment of the initial model of the marine oil spill system. The following factors, the edge contour characteristics of the experimental perimeter, the area change with time, the melting rate, the irregular image contour, *etc*., are analyzed at the same time. Then the model was further mapped to the establishment of the marine oil spill model based on the LSTM network. The dynamic behavior of

Table 1. *The numerical relationship between* V_w, V_F, α, I, C, β *of the system model.*

Cm	V_w	V_f	α	β
I	(+)	0	(≈2.14)†	(≈2.34)‡
	(+)	(+)	(≈2.38)	(≈4.84)
	(+)	(–)	(≈1.56)	2.41
C	(+)	0	(≈2.77)‡	(≈2.35)
	(+)	(+)	(≈2.95)	(≈5.23)‡
	(+)	(–)	(≈1.72)	2.65

†*When the rate is changed, it is basically unchanged.*
‡*Changes a lot when the speed changes.*

the data is predicted, and the fitting curve of the test image data is obtained, which verifies the feasibility of the method. The actual melting rate of silicon dioxide is estimated based on the edge profile parameters. Some images have lower original pixels, blurred boundary features, and assumptions in the experimental model, so there are more data materials to be studied in the 2D time series images. To better describe the characteristics of silicon dioxide's profile, the factors that affect the edge, shape (F), perimeter (L), area (S), and diffusion rate (Vx) were selected as parameters. The former adopts the method of data calculation, whereas this paper adopts the intervention of random factors. In the process of neural network learning, the correlation between $[T-1, t+1]$ can be analyzed, and the weight value of different influencing factors can be automatically modified to simplify the process of trajectory prediction. The training model has portability. After transfer learning, more and more training data will eventually enhance the anti-interference ability of the model, some problems also occur. In the model training process, in addition to the wind and flow processes, this paper should also add the other three aspects of the process research, which will make the results more accurate. Combining the advantages and disadvantages of the two models, a comprehensive prediction model of oil spill trajectory can be proposed in further research.

Numerical Model Validation

In the past, when researchers analyzed the effect of wind and ocean currents on oil spills, they often set a commonly used empirical wind influence factor (Hoang, Pham, and Nguyen, 2018; Lee, Kim, and Kim, 2017). Regarding the interaction of wind and ocean currents on the oil spill trajectory, simulation experiments in the tidal wind flume show that different relative speeds will have different effects on the expansion and deviation of oil particles. The experiment should select the appropriate edge expansion displacement factor α and edge drift rate factor β based on the relative velocity of wind V_w and current V_F in Δt. Combined with the mathematical model in this paper, the relationships among V_w wind speed, V_F water speed, edge expansion displacement factor α, instantaneous oil spill I, continuous oil spill C, and edge drift rate factor β are shown in Table 1.

Figure 7 shows a stacked polyline of silicon dioxide melting over time. Taking the space vector point of the established dynamic grid reference system as the origin of the coordinates, ignoring the microboundaries of the particles, the outline of the particles in the collected picture is shown. The outline of all the pictures and all the obtained particle information are integrated to obtain the movement track of the silicon dioxide particles.

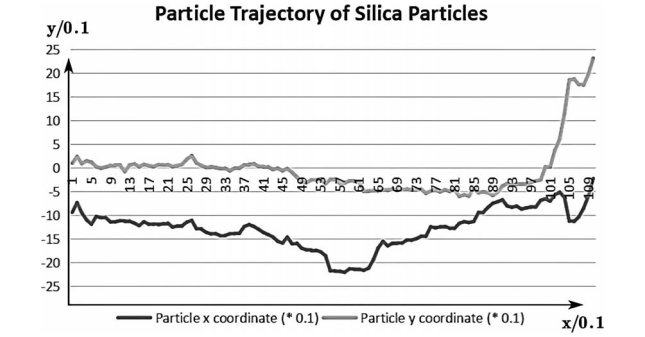

Figure 7. A stacked polyline of silicon dioxide melting over time. These lines show the change process of the mass center of the object in the initial model. It is important to grasp the overall transfer path of the whole oil spill material in time in the process of monitoring the oil spill on the sea, which is important to predict the scope of the oil spill process and the entire oil spill accumulation area.

Figure 8 shows a time-varying scatter plot of area and perimeter. Through the analysis of the 2D time series image database, the Matplotlib module in Python is used to establish a data scatter plot to obtain the relevant edge contour parameters.

This same type of experiment can be compared with the establishment of a model of an oil spill accident at sea. Figure 8

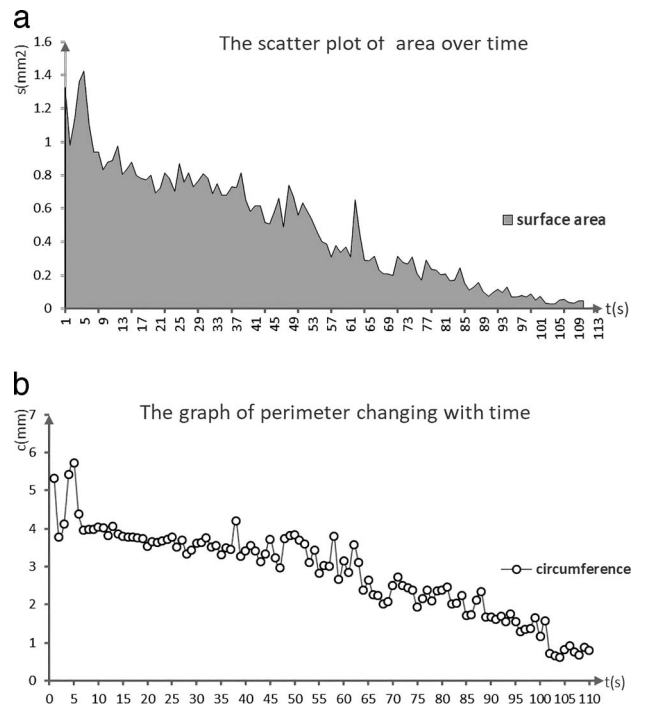

Figure 8. A time-varying scatter plot of area (A) and perimeter (B). These two pictures show the change trend of area and perimeter with time in the initial model. As an imaginary inverse process, the transformation law of perimeter and area can play an important role in the prediction of oil spill radius and oil spill edge characteristics of the oil spill model from the geometric point of view.

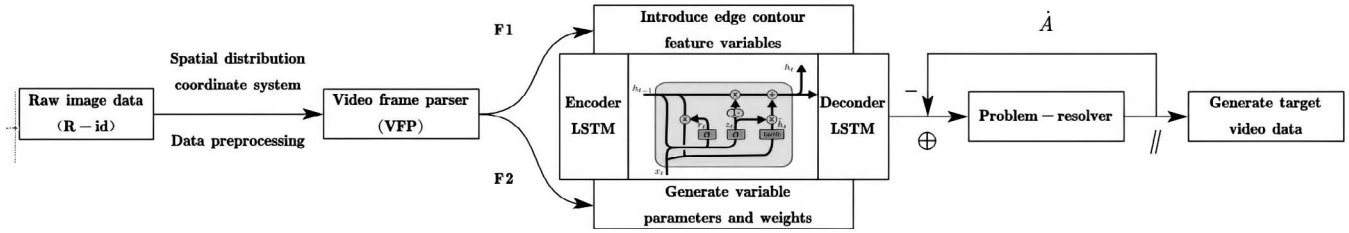

Figure 9. Schematic diagram of realizing the operation process of the oil spill system based on deep learning. As the framework of the whole monitoring system, this paper simply shows readers the prediction process of oil spill dynamic behavior under the action of neural network and responds quickly to the change of oil spill state from the macroscopic and geometric perspectives, which is also the advantage of the whole system.

shows that with the continuous melting of silicon dioxide under high temperature environment, its shape is irregular and shows an overall decreasing trend, and the area gradually decreases but the circumference shows obvious fluctuations. Non-uniformity reduction occurs, but the total will gradually decrease with the reduction of solids. Due to the irregular change in concentration during oil spill, the circumference and area increase irregularly, resulting in the change of color depth on the satellite real-time image and the effect on the oil diffusion rate.

The preprocessing of 2D image data is as follows. For the 2D time series image given by the subject, plus the silicon dioxide mentioned in the modeling assumption comprising non-uniform unit substances, the area was calculated by the image-based silicon dioxide fusion characterization model constructed in this paper. The area is proportional to the volume of the particle:

$$V_{(x)} = \delta * \lim_{i \to \infty} \sum_{i=1}^{\beta} (\Delta f(x_i) * h_i * \theta), \tag{10}$$

where, δ is the volume uniformity coefficient.

The results of this experiment show that the melting rate of silicon dioxide is proportional to the volume, that is $m = \alpha \times \Delta V$, where α is the mass uniformity coefficient, and then the area characteristic index set by the second question can be used to help the Matplotlib tool of Python 3.7.1 learn the differential relationship of m-t to obtain a m-v curve. As shown Figure 8, the melting speed of the model is $0.96 \times 10^{-2} \times \lambda\alpha$. Among them, $\lambda\alpha$ is a known constant for system monitoring.

Figure 9 shows the prediction model of behavioral dynamics and the overall process of the model. The original video data obtained in real time is preprocessed, and the rate of change of the spatial distribution is used for estimation and prediction, while the time delay caused by the use of original data processing was attempted to be avoided to improve the system response time. The preprocessed experimental data obtained by the system is subjected to cyclic neural network learning, and the data is transmitted and processed through the gates of the input gate, the forget gate, and the output in the LSTM so that the historical information fragments can be remembered for a long time. Target video information was generated from original data through the establishment of spatial distribution coordinate system, video frame parser (VFP), decoder-encoder, and other modules.

Figure 10 shows the topology of the LSTM network model system. The system model uses two channels of raw data and preprocessed data as the input layer of the entire experiment, which greatly improves the calculation efficiency and accuracy of channel extraction and reduces the analysis error caused by single data input. The FC layer is a fully connected layer. When the output video information can be flattened, it can be directly connected to the output layer instead of passing through the fully connected layer. It can learn the nonlinear combination parameter characteristics required by some models in a relatively simple way. Therefore, this method is used to learn all the required weight values and to establish all relevant edge feature relationships to integrate the features required by the eligible model while reducing the proportion of features with lower actual relationship with the model to improve the

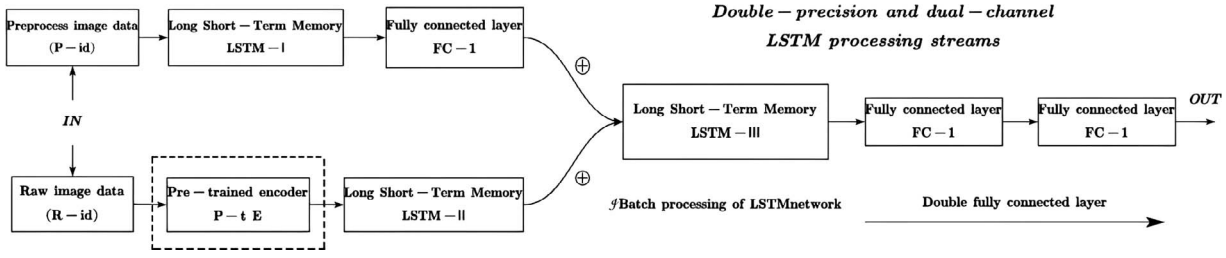

Figure 10. The topology of the LSTM network model system. Different from Figure 9, the internal part of the model structure of the oil spill prediction system is shown. The neural network and the information memory function of LSTM are introduced to realize the trend prediction of the oil spill state at the initial stage of oil spill. Compared with other models, it has a higher fault tolerance rate and better effect.

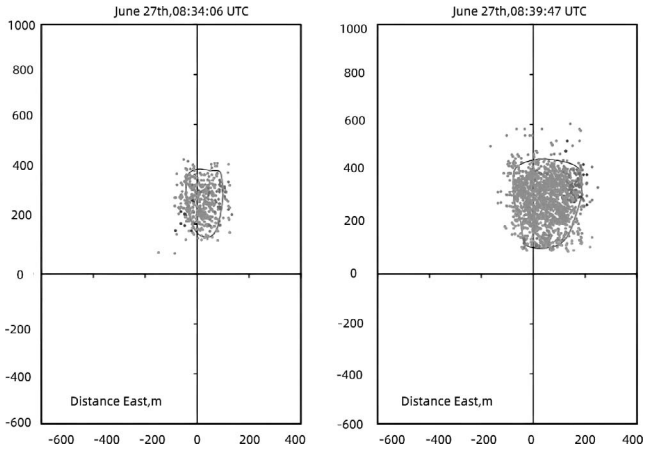

Figure 11. The area enclosed by the solid line represents the smooth contour obtained from the photograph taken in the marine diesel-natural gas test. The light-shaded elliptical set represents the simulated prediction results of the oil spill trajectory (0834:06–0839:47, 27 June).

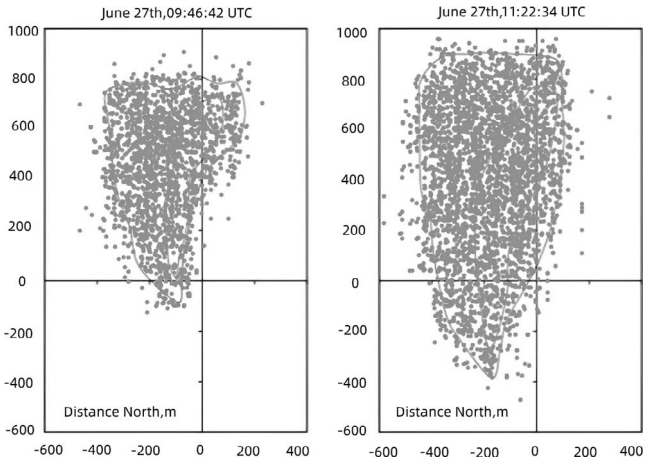

Figure 12. The area enclosed by the solid line represents the smooth contour obtained from the photograph taken in the marine diesel-natural gas test. The light-shaded elliptical set represents the simulated prediction results of the oil spill trajectory (0911:36–1351:58, 29 June).

learning model reliability. Here, $P - tA$ is used as a pretraining encoder on the second chain. The purpose is to seek the initial value of the network weight to provide better optimization capabilities and to reduce generalization and training errors. In the model of dynamic video processing, a large number of neurons are required based on the LSTM network algorithm. Because the model has relevant features with low weight and local connection, the topology using two fully connected layers can indirectly increase the number of neurons.

When the test oil leaks into the relevant sea area, the method of projecting the velocity vector to zero outside the normal direction of the boundary is usually used to address the boundary conditions. Figures 11 and 12 are the smooth aviation oil spill profiles and the regional prediction results of oil spill impact of the DeepSpill test from 0834 to 1357 on 27 June.

In Figure 11, the area enclosed by the solid line represents the smooth contour obtained from the photograph taken in the marine diesel-natural gas test. The light-colored elliptical set represents the simulated prediction results of the oil spill trajectory (0834:06–0839:47, 27 June).

In Figure 12, the area enclosed by the solid line represents the smooth contour obtained from the photograph taken in the marine diesel-natural gas test. The light-colored elliptical set represents the simulated prediction results of the oil spill trajectory (0911:36–1351:58, 29 June).

DISCUSSION

The offshore oil spill emergency system is a relatively large operation group. The LSTM network can be used to learn different weight parameters for edge contour features such as real-time terrain, wind speed, concentration, *etc.*, to more realistically approximate the actual situation and predict more stable oil spill behavior change trend. The proposed model uses a dual-channel input mode to reduce the calculation error caused by a single factor. At the same time, it reduces the proportion of features that are less related to the model to increase the reliability of model learning. Several edge contour features need to be considered—shape (F), perimeter (L), concentration (Cb), diffusion rate (Vx), area (Sv), *etc.*—and this paper mainly refers to the simulation object with the change of shape as the focus. The change of shape is relatively easy to obtain. For the analysis of the change of the total oil spill and the type of oil spill, including the distribution of oil film, the loss of settled oil, and the eight dynamic processes of dirty oil. The analysis will wait for the past data of special instrument sensors and serve as the input of the entire monitoring system. Through learning the training data, the weight parameters will be continuously modified to achieve progressive improvement of the monitoring system.

The data preprocessing of the oil spill dynamic prediction model uses the spatial distribution variable preprocessing of the dynamic grid reference system as the system input, which can well avoid the prediction offset problem caused by the delay of the multisensor processing of the original data. The LSTM network uses a control gate to control the part that needs to be memorized to remove or add information to the cell state. By continuously acquiring test image data to learn and modify the system model, it can finally predict the behavior of marine oil spills.

For the prediction maps shown in Figures 11 and 12, the prediction range will be larger than the actual one. This is because the main body of the oil spilled, in addition to its own expansion in the marine environment and in addition to drift, evaporation, emulsification, and sinking also occurring, so that the amount of oil spilled on the ocean surface is gradually reduced, and the correlation between particles is ignored in the randomness calculation through the random factor, thereby magnifying the predicted image range of oil spill. In the process of system optimization, the reinforcement training algorithm should be better combined to simulate the required training data to reduce human error.

At the same time, it can be seen from the figure that the assumed coverage of the oil particle model is low when t is small, and the coverage of the later oil particle model gradually increases with time. This is because with the increase of t, the weight information is more accurate, and the error rate is smaller. The appearance of this situation is very consistent with the fitting characteristics and learning rules of deep learning. This method is relatively simple and has a high fault tolerance. It can be used as an oil spill auxiliary system. It can also calculate and predict the oil spill trajectory and the sensitive area of the oil spill effect in a short time, which provides a basic basis for the handling and decision-making of offshore oil spill accidents.

CONCLUSIONS

By establishing a dynamic behavior prediction model for offshore oil spills based on deep learning, the image data processing and dynamic prediction of edge contour feature input are performed through the LSTM deep dual-channel network, and the weight coefficients are continuously changed to improve the memory update speed. In this model, the proportion of contour shape and perimeter is strengthened, and the weight of other factors is reduced. The experimental data shows that the prediction error of the real image data and the fitting curve obtained by predicting the experimental data of the detection image indicate that the experimental error of the feature data is within a reasonable error range. It also proves that the LSTM network has many advantages as a special existence in the RNN, which does not exist in the general RNN. The LSTM can learn graphic data-containing noise in the real environment with good stability and can provide reliable interactive prediction. The robustness of the system after special pretreatment can minimize human errors and cost and provide a good auxiliary monitoring effect for the oil spill emergency warning system. This model is used in the real-time monitoring auxiliary system of oil spill diffusion, which can improve the reliability of oil leakage early-warning during movement. As an oil spill early-warning auxiliary system, the model has a high fault tolerance rate. Although certain errors occur in the experimental results, it can reflect the main characteristics and show strong stability in general, and the wind and current data can be obtained directly through the sensor. It is relatively simple to predict the dynamic trajectory of oil spill behavior, which provides a more suitable solution for taking measures to block and recover oil spills. In addition, to better reflect the feedback of more factors to the oil spill action, the influence of factors such as concentration and type on the time series of oil spill behavior should be further studied.

ACKNOWLEDGMENTS

This work was supported in part by the National Natural Science Foundation of China Grants 51709032, 61802043, and 62002043; by the Liaoning Revitalization Talents Program Grant XLYC1908007; by the Foundation of Liaoning Key Research and Development Program Grant 201801728; by the Fundamental Research Funds for the Central Universities Grant 3132016352; and by the Dalian Science and Technology Innovation Fund Grants 2018J12GX037 and 2019J11CY001.

LITERATURE CITED

Abascal, A.J.; Castanedo, S.; Núñez, P.; Mellor, A.; Clements, A.; Pérez, B., and Medina, R., 2017. A high-resolution operational forecast system for oil spill response in Belfast Lough. *Marine Pollution Bulletin*, 114(1), 302–314.

Alpers, W.; Holt, B., and Zeng, K., 2017. Oil spill detection by imaging radars: Challenges and pitfalls. *Remote Sensing of Environment*, 201, 133–147.

Bhangale, U.; Durbha, S.S.; King, R.L.; Younan, N.H., and Vatsavai, R., 2017. High performance GPU computing based approaches for oil spill detection from multi-temporal remote sensing data. *Remote Sensing of Environment*, 202, 28–44.

Chiri, H.; Abascal, A.J.; Castanedo, S., and Medina, R., 2019. Mid-long term oil spill forecast based on logistic regression modelling of met-ocean forcings. *Marine Pollution Bulletin*, 146, 962–976.

Ding, S.; Wang, Z.; Peng, Y.; Yang, H.; Song, G., and Peng, X., 2017. Dynamic prediction of the silicon content in the blast furnace using LSTM-RNN based models. *Proceedings of the 2017 International Conference on Computer Technology, Electronics and Communication (ICCTEC)*, pp. 227–231.

Garcia-Pineda, O.; Holmes, J.; Rissing, M.; Jones, R.; Wobus, C.; Svejkovsky, J., and Hess, M., 2017. Detection of oil near shorelines during the Deepwater Horizon oil spill using synthetic aperture radar (SAR). *Remote Sensing*, 9(6), 567.

Garcia-Pineda, O.; Hu, C.; Sun, S.; Garcia, D.; Cho, J.; Graettinger, G., and Ramirez, E., 2019. Classification of oil spill thicknesses using multispectral UAS And satellite remote sensing for oil spill response. *Proceedings of the IGARSS 2019-2019 IEEE International Geoscience and Remote Sensing Symposium*, pp. 5863–5866.

Hoang, A.T.; Pham, V.V., and Nguyen, D.N., 2018. A report of oil spill recovery technologies. *International Journal of Applied Engineering Research*, 13(7), 4915–4928.

Hou, Y.; Li, Y.; Liu, Y.; Li, G., and Zhang, Z., 2019. Effects of polycyclic aromatic hydrocarbons on the UV-induced fluorescence spectra of crude oil films on the sea surface. *Marine Pollution Bulletin*, 146, 977–984.

Jeong, Y.; Kim, S., and Yi, K., 2020. Surround vehicle motion prediction using LSTM-RNN for motion planning of autonomous vehicles at multi-lane turn intersections. *IEEE Open Journal of Intelligent Transportation Systems*, 1, 2–14.

Ji, H.; Xu, M.; Huang, W., and Yang, K., 2020. The influence of oil leaking rate and ocean current velocity on the migration and diffusion of underwater oil spill. *Scientific Reports*, 10(1), 9226.

Kasimu, A.; Wu, D.D., and Bian, Y., 2019. System dynamic-based oil weathering processes: Simulation and analysis. *IEEE Systems Journal*, 14(1), 1375–1383.

Lee, C.J.; Kim, G.D., and Kim, Y.H., 2017. Performance comparison of machine learning based on neural networks and statistical methods for prediction of drifter movement. *Journal of the Korea Convergence Society*, 8(10), 45–52.

Mao, W.; Liu, M.; Salzmann, M., and Li, H., 2019. Learning trajectory dependencies for human motion prediction. *Proceedings of the IEEE International Conference on Computer Vision*, pp. 9489–9497.

Mansur, L. and Price, D.M., 2019. 17 OIL-RW: A mathematical model for predicting oil spills trajectory and weathering. *Hydraulic and Environmental Modelling: Proceedings of the Second International Conference on Hydraulic and Environmental Modelling of Coastal, Estuarine and River Waters*. Volume I. New York: Routledge, pp. 45–56.

Mirnaghi, F.S.; Pinchin, N.P.; Yang, Z.; Hollebone, B. .; Lambert, P., and Brown, C.E., 2019. Monitoring of polycyclic aromatic hydrocarbon contamination at four oil spill sites using fluorescence spectroscopy coupled with parallel factor-principal component analysis. *Environmental Science: Processes and Impacts*, 21(3), 413–426.

Murawski, S.; Schlüter, M.; Paris-Limouzy, C.B., and Aman, Z.M., 2019. Resolving the dilemma of dispersant use for deep oil spill response. *Environmental Research Letters*, 14(9), 7–12.

Naidu, V.S.; Sukumaran, S.; Dubbewar, O., and Reddy, G.S., 2013. Operational forecast of oil spill trajectory and assessment of

impacts on intertidal macrobenthos in the Dahanu region, west coast of India. *Journal of Coastal Research*, 29(2), 398–409.
Nhat, D.M.; Venkatesan, R., and Khan, F., 2020. Data-driven Bayesian network model for early kick detection in industrial drilling process. *Process Safety and Environmental Protection*, 138, 130–138.
Pisano, A.; De Dominicis, M.; Biamino, W.; Bignami, F.; Gherardi, S.; Colao, F., and Zambianchi, E., 2016. An oceanographic survey for oil spill monitoring and model forecasting validation using remote sensing and in situ data in the Mediterranean Sea. *Deep Sea Research Part II: Topical Studies in Oceanography*, 133, 132–145.
Santiago, A.; Dorronsoro, B.; Nebro, A.J.; Durillo, J.J.; Castillo, O., and Fraire, H.J., 2019. A novel multi-objective evolutionary algorithm with fuzzy logic based adaptive selection of operators: FAME. *Information Sciences*, 471, 233–251.
Sari, D.K.; Wulandari, D.P., and Suprapto, Y.K., 2019. Training performance of recurrent neural network using RTRL and BPTT for gamelan onset detection. *Journal of Physics Conference Series*, 1201, 012046.
Wang, Y.; Zhu, S., and Li, C., 2019. Research on multistep time series prediction based on LSTM. *Proceedings of the 2019 3rd International Conference on Electronic Information Technology and Computer Engineering (EITCE)*, pp. 1155–1159.
Xiong, Y. and Zhou, H., 2019. Oil spills identification in SAR image based on convolutional neural network. *Proceedings of the 2019 14th International Conference on Computer Science and Education (ICCSE)*, pp. 667–670.
Yankelovich, A. and Spitzer, H., 2019. Predicting illusory contours without extracting special image features. *Frontiers in Computational Neuroscience*, 12, 106.
Yapa, P.D., 1996. State-of-the-art review of modeling transport and fate of oil spills. *Journal of Hydraulic Engineering*, 122(11), 549–609.
Yu, Y., 2019. Comments on "Virtual Simulation of Pollution Diffusion in Oil Pollution Accidents." *Ekoloji*, 28(108), 997–1001.
Zhang, L.J.; Huang, X.D.; Wang, Y.; Wang, C.Y., and Sun, Y.Z., 2019. Discussion on dual–tree complex wavelet transform and generalized regression neural network based concentration-resolved fluorescence spectroscopy for oil identification. *Analytical Methods*, 11(36), 4566–4574.
Zhang, Y.; Zhu, J.; Peng, Y.; Pan, J., and Li, Y., 2020. Experimental research of flow rate and diffusion behavior of nature gas leakage underwater. *Journal of Loss Prevention in the Process Industries*, 104119.